

**NACA**

0143532

TECH LIBRARY KAFB, NM

# RESEARCH MEMORANDUM

PHOTOGRAPHIC STUDY OF COMBUSTION IN A ROCKET ENGINE

I - VARIATION IN COMBUSTION OF LIQUID OXYGEN AND  
GASOLINE WITH SEVEN METHODS OF  
PROPELLANT INJECTION

By Donald R. Bellman and Jack C. Humphrey

Flight Propulsion Research Laboratory  
Cleveland, Ohio

CLASSIFIED DOCUMENT

This document contains classified information  
the National Defense of the United  
the meaning of the Espionage Act,  
its transmission or the  
revelation of its contents in any manner to an  
unauthorized person is prohibited by law.  
Information may be imparted  
only to persons in the Army and naval  
services of the United States, appropriate  
civilian officers and employees of the Federal  
Government who have a legitimate interest  
therein, and to United States citizens  
loyalty and discretion who of necessity  
are informed thereof.

TECHNICAL  
EDITING  
WAIVED

**NATIONAL ADVISORY COMMITTEE  
FOR AERONAUTICS**

WASHINGTON

August 26, 1948

**CONFIDENTIAL**

319.98/13



0143532

NACA RM No. ESF01

## NATIONAL ADVISORY COMMITTEE FOR AERONAUTICS

RESEARCH MEMORANDUM

## PHOTOGRAPHIC STUDY OF COMBUSTION IN A ROCKET ENGINE

## I - VARIATION IN COMBUSTION OF LIQUID OXYGEN AND

## GASOLINE WITH SEVEN METHODS OF

## PROPELLANT INJECTION

By Donald R. Bellman and Jack C. Humphrey

## SUMMARY

Motion pictures at camera speeds up to 3000 frames per second were taken of the combustion of liquid oxygen and gasoline in a 100-pound-thrust rocket engine. The engine consisted of thin contour and injection plates clamped between two clear plastic sheets forming a two-dimensional engine with a view of the entire combustion chamber and nozzle. A photographic investigation was made of the effect of seven methods of propellant injection on the uniformity of combustion.

From the photographs, it was found that the flame front extended almost to the faces of the injectors with most of the injection methods, all the injection systems resulted in a considerable nonuniformity of combustion, and luminosity rapidly decreased in the divergent part of the nozzle. Pressure vibration records indicated combustion vibrations that approximately corresponded to the resonant frequencies of the length and the thickness of the chamber. The combustion temperature divided by the molecular weight of the combustion gases as determined from the combustion photographs was about 50 to 70 percent of the theoretical value.

## INTRODUCTION

As part of a basic study of rocket combustion, an investigation is being conducted at the NACA Cleveland laboratory to evaluate photographically rocket-design variables and to obtain an insight into the causes of combustion vibrations and asymmetric thrust. Such fundamental information is needed to provide a sound basis for designing propellant injectors, combustion-chamber volumes and shapes, and cooling systems.

The technique of photographing combustion has been used by several laboratories including the General Electric Company, the M. W. Kellogg Company, the Aerojet Engineering Corp., and the Jet Propulsion Laboratory of the California Institute of Technology. In most of the investigations, the combustion chamber was a small tube and the transparent material was glass or quartz.

The photographic technique developed at the NACA Cleveland laboratory and applied to a 100-pound-thrust rocket engine from September to December 1947 for the investigation had three important features: (1) The entire combustion chamber and the nozzle were photographed; (2) the combustion chamber and the nozzle were of uniform thickness to eliminate the effect of nonuniformity of thickness on luminosity; and (3) a low melting-point material was used for the sides to prevent the transparent material from becoming luminous and obscuring the combustion pattern.

Motion pictures of combustion in the 100-pound-thrust rocket engine were taken at camera speeds up to 3000 frames per second. Runs were made to determine the effect of seven methods of propellant injection on the combustion of liquid oxygen and gasoline and the results are reported. The results are most favorably observed as a motion picture projected at normal speeds, thus presenting the results as slow motion pictures.

### APPARATUS

#### Combustion Chamber and Nozzle

An assembled and an unassembled view of the transparent-sided rocket engine is shown in figure 1. The rocket engine consists of contour plates and an injection plate having sheets of transparent material held to both sides by means of suitable spacer blocks and clamping frames. The contour plates were copper with chromium plating on the inner surface to reduce erosion by the combustion gases. For most of the experiments, the transparent sides were made from methylmethacrylate, which is a clear plastic. This material, like quartz, has excellent resistance to thermal shock but for the application of combustion photography it is superior to quartz because the low melting point of the plastic prevents the walls from becoming luminous and obscuring the combustion pattern. The low melting point of the plastic, however, limits the useful duration of the runs to a few seconds. Plate glass was used for some of the preliminary experiments but was unsatisfactory because of low resistance to thermal shock and luminosity at high temperatures.

Each side of the rocket consisted of an inner sheet of 1/4-inch-thick plastic, which was backed with a 3/4-inch-thick sheet of plastic in order to withstand the combustion pressures. The transparent sheets were sealed to the contour plates with asbestos-type sheet packing.

The combustion chamber including the nozzle had a uniform thickness of 1/2 inch and was designed to produce 100 pounds of thrust with a combustion-chamber pressure of 300 pounds per square inch absolute. The characteristic length (combustion-chamber volume divided by throat area) was about 60 inches. The rocket engine was mounted at a downward angle of 45° to prevent the accumulation of propellants in the chamber in the event of an ignition failure. A combustion pressure tap and vibration pickup were installed through one of the contour plates at about midpoint of the combustion chamber.

### Injectors

The seven injection systems that were used for injecting the propellants (liquid oxygen and gasoline) are diagrammatically shown in figure 2.

The first type of injection system, single intersecting jets, has single jets of each propellant directed at 45° to the center line of the chamber. The jets start near the two ends of the injection plate and intersect on the center line of the engine about  $1\frac{1}{4}$  inches from the injection plate. For the operating conditions used, the difference in momentum of the two streams would cause a resultant combined stream to be deflected about 12° from the center line toward the gasoline-injection side (lower side) of the rocket engine. A photograph of the contour and injection plates with this type of injector is shown in figure 3.

The second injection system is the same as the first system except that two turbulence projections are attached to the chamber walls about  $3\frac{3}{4}$  inches from the injection plate to provide a constriction for producing turbulence. These projections made a constriction area of one-half the normal cross-sectional area.

The third injection method, multiple intersecting jets, is similar to the first system except that six parallel jets of each propellant replace the single jet. The jets were also directed

at  $45^\circ$  to the center line and again the operating conditions used cause a resultant combined stream to be deflected  $12^\circ$  towards the gasoline-injection side of the combustion chamber.

The fourth injection method is similar to the third system except for the addition of turbulence projections as in the second system. The contour and the injection plates with the multiple intersecting jets and the turbulence projections are shown in figure 4.

The Enzian system, which was named after the German rocket in which it was first used, was the fifth type of injection system. This system consists of single jets of each propellant impinging at a common spot on an angular plate projecting into the chamber. One projecting plate and set of propellant jets were placed on each side of the rocket engine with the igniting flame in the center. Figure 5 shows the contour and the injection plates for the Enzian method of injection.

The impingement plates were removed from the Enzian system to form the sixth injection method, which will be called two pairs of intersecting jets. The propellant streams were directed toward each other at an angle of  $30^\circ$  with the center line of the engine and intersected at a point about  $3/8$  inch from the surface of the injector.

The seventh injection method was a premixing type in which the propellants were mixed just before injection into the combustion chamber through a tube having an orifice at the chamber end.

#### Igniter

The propellants in the early runs were ignited by means of a gaseous oxygen - alcohol flame which, in turn, was ignited by a spark plug. The rocket with this igniter attached is shown in figures 1 and 3. The apparatus did not function properly and frequently burned out. Later gunpowder squibs were commercially obtained and used for ignition. These squibs were electrically ignited and produced a flame about 1 foot in length and had a burning time of about 4 seconds. Figures 4 and 5 show the squib holder attached to the injection plate. The gunpowder squib was found to be a satisfactory ignition method and was used for all subsequent runs.

### Propellant Systems

A schematic diagram of the rocket engine with auxiliary apparatus is shown in figure 6. The gasoline in tank II was pressurized to 20 pounds per square inch by nitrogen from regulator FF in order to minimize cavitation in the inlet to the pumps. From the tank, the gasoline flowed through rotameter O to two four-cylinder, positive-displacement pumps DD, which were coupled to a single motor EE. The eight pumping strokes were uniformly staggered to produce a minimum flow variation. From the pump, the gasoline passed through a series of hydraulic resistances BB to eliminate pulsations. The gasoline then flowed either through propellant control valve Z and into combustion chamber V or through relief valve CC and back into the supply tank. During a run, a pressure of about 400 pounds per square inch was required to send the fuel into the combustion chamber and the relief valve was set at a pressure of 900 pounds per square inch so that no fuel was bypassed when the propellant control valve Z was open.

The liquid oxygen was stored in a 4-gallon stainless-steel tank I located close to the combustion chamber. The tank was pressurized to 400 pounds per square inch by means of gaseous oxygen from pressure-reducing valves A and B. From the tank, the liquid oxygen flowed through a vane-type flowmeter T and propellant control valve X to combustion chamber V.

In order to stop the combustion quickly after each run, flushing the liquid-oxygen line with nitrogen was necessary. This flushing was accomplished by pressurizing tank AA with nitrogen during the run by means of the three-way solenoid valve F. At the conclusion of each run, the three-way solenoid valve sent the contents of tank AA into the liquid-oxygen line close to the injector, which forced any oxygen remaining in the line out through valve U.

### Instrumentation

The thrust stand was of the horizontal parallelogram type with the horizontal component of the thrust acting on a bar spring equipped with strain gages. The strain gages were connected to a self-balancing resistance-bridge instrument that recorded on a strip chart. The thrust apparatus was calibrated with a bell crank and a platform scale and was accurate to less than 1 percent.

Combustion-chamber pressure vibrations were picked up with a commercial engine knock indicator of the magnetostriction type and, because it was a rate-of-change-type instrument, absolute pressures could not be measured with it. The indicator was connected to an oscilloscope and a record was obtained on a strip of 35-millimeter film.

All pressures were measured with standard gages having an accuracy of about 2 percent. The fuel rotameter was so calibrated that corrected readings were accurate within 1/2 percent. The liquid-oxygen flowmeter was accurate to about 7 percent.

All of the measurements except thrust and pressure vibrations were recorded by photographing an instrument panel with a camera at a rate of 3 frames per second. The camera produced a 5-by-5-inch negative from which the various instruments were directly read. The following measurements were taken in this manner: combustion-chamber pressure, liquid-oxygen-nozzle pressure, gasoline-nozzle pressure, liquid-oxygen-tank pressure, gasoline-pump pressure, liquid-oxygen flow, gasoline flow, and time.

#### Combustion Camera

The combustion photographs were taken with a 16-millimeter commercial motion-picture camera having a maximum speed of 3000 frames per second. The camera held 100 feet of film, which allowed an operating time of about  $2\frac{1}{2}$  seconds. The film began from rest at the start of the run and about two-thirds of the film was used before the camera attained maximum speed. An electronic-wave generator that maintained a constant frequency of 1000 cycles per second was used to mark the film every 1/1000 second. The camera was placed inside a strong steel box to protect it from damage in case of a chamber explosion. The photographs were taken through a thick plastic window mounted on the end of the steel box.

## OPERATING CONDITIONS AND PROCEDURE

Commercial liquid oxygen and 62-octane unleaded gasoline were used for all runs. The theoretical performance for this propellant combination has been calculated as follows:

Maximum specific impulse, lb-sec/lb . . . . .	242
Oxidizer-fuel weight ratio for maximum specific impulse . . . . .	2.5
Stoichiometric oxidizer-fuel weight ratio . . . . .	3.5
Ratio of specific heats for oxidizer-fuel weight ratio of 2.5 . . . . .	1.22
Combustion temperature at oxidizer-fuel weight ratio of 2.5, °R . . . . .	5900

These theoretical calculations were made for a combustion-chamber pressure of 300 pounds per square inch absolute; the transparent-sided rocket engine was designed to produce 100 pounds of thrust at this combustion-chamber pressure. When a specific impulse of 180 pound-seconds per pound and an oxygen-fuel weight ratio of 2.5 were assumed, an oxygen flow of 0.40 pound per second and a fuel flow of 0.16 pound per second would be required to produce the 100 pounds of thrust. An attempt was made to maintain these flow rates for all the runs.

High-speed motion pictures were taken of combustion and performance data recorded when the transparent-sided rocket was operated with each of the seven injection methods previously described. In operation, the liquid-oxygen flow was started first and then about 15 seconds was allowed for the oxygen to cool the lines and the injectors and to reach the proper flow rate. The high-speed camera was then started simultaneously with the ignition of the squib. After a delay of 1 second to allow the camera to reach a suitable speed, the fuel was admitted and combustion started. As soon as all the film in the camera was exposed, the propellant flow was stopped and the liquid-oxygen line was flushed with nitrogen.

All of the firing operations including shutoff were automatically performed and were started with the closing of a single switch. Because the camera operated less than 3 seconds, each run lasted about  $1\frac{3}{4}$  seconds. After each run the inner sheets of the transparent sides and the squib were replaced.



## RESULTS

## General Performance Data

The experimental and the calculated data for 19 runs made with the transparent-sided rocket engine are presented in table I. The photographically recorded data given in this table are those from the frame showing the highest combustion-chamber pressure for the run. The time during the run that this frame was taken approximately corresponds to the peak thrust. During a few runs, no combustion-chamber-pressure reading was obtained and for these runs the data taken about 1 second after the start are shown. The material burned from the plastic walls was not considered when the specific-impulse calculations were made. The loss in weight of the plastic walls in the combustion-chamber section was estimated at 15 to 20 percent of the total propellant flow. Considerable variation exists in the performance between repeated runs as well as between runs having different injection systems. These variations could be caused by any or all of the following conditions: (1) inaccuracy of the instrumentation caused by rapid changes in measured quantities, (2) variation in the propellant flows, and (3) variations in the rate of wall decomposition and throat enlargement. During each run, the plastic sides at the throat burned away to a depth of about  $1/4$  inch, whereas elsewhere only about  $1/16$  inch of material disappeared. The rapid enlargement of the throat prevented stable conditions from being reached and caused the thrust and the combustion-chamber pressure to decrease rapidly after reaching a maximum. Because stable conditions were never attained, the accuracy of thrust, combustion-chamber pressure, and other measurements was reduced.

## Observations from Combustion Photographs

Starting characteristics. - At the start of most runs, a small flame appeared in the vicinity of the intersection of the propellant jets. This flame swelled and diminished in an irregular and uneven manner during the time it was extending to fill the combustion chamber. In many runs about  $1/2$  second was required for the flame to fill the entire chamber and to become relatively stable. In several runs in which the squib was fired simultaneously with the admission of the fuel instead of 1 second earlier, the start consisted of a series of explosions occurring throughout the entire chamber. Figure 7 shows a sequence of pictures from such a run. In these cases, stable combustion was sometimes attained in as little as  $1/10$  second but frequently the transparent sides failed to withstand the explosions.

Single intersecting jets. - When the single intersecting jets were used without the turbulence projections, combustion took place throughout the entire chamber but nonluminous pockets repeatedly appeared near the intersection of the jets and flowed toward the nozzle along the center line. A series of frames showing a typical nonluminous pocket as it flowed toward the nozzle is shown in figure 8. There was no uniformity in successive pockets, which appeared at irregular intervals. The pockets all moved at about the same rate, however, and remained in the middle section of the chamber.

Single intersecting jets with turbulence projections. - The addition of the turbulence projections to the rocket engine equipped with the single intersecting jets eliminated the nonluminous pockets that flowed along the center line and created a tendency for a stationary pocket to be formed along the upper edge between the turbulence projection and the nozzle. Figure 9 shows combustion under such conditions. For run 3, the two corners near the injection plate were inadvertently blocked out by a gasket on the outside of the combustion chamber.

Multiple intersecting jets. - The multiple intersecting jets when used without the turbulence projections tended to create nonluminous pockets along the upper and lower edges of the chamber and in the vicinity of the injectors. Frames from three runs with this injection system are shown in figure 10. The photographs from runs 7 and 8 show typical configurations of the flame. There is a large dark area in the vicinity of the injectors and the flame does not closely follow the edges of the chamber. The photographs from run 10 show a configuration that was obtained in only one out of six runs with this type of injection. Here the flame extends to the injector faces.

Multiple intersecting jets with turbulence projections. - The use of the turbulence projections with multiple intersecting jets caused the combustion to take place much more uniformly throughout the chamber. In general, the flame extended to the injectors and to the chamber edges in most places. Photographs from two such runs are shown in figure 11. Run 12 had a high thrust (113 lb) and the flame appeared to be unusually uniform throughout. Run 14 had some dark areas, which were probably caused by the low oxygen flow, and the thrust (72 lb) was quite low. It is thus indicated that the turbulence projections had a different effect with the multiple jets than with the single jets. The use of the turbulence projections with the single intersecting jets caused the combustion to be less uniform and to break away from the wall in places, whereas the use of the turbulence projections with the multiple jets tended to eliminate the dark areas along the edges and near the injectors.

Enzian-type injection. - Combustion with the Enzian-type injector, which has jets of each propellant impinging on a projection, is shown in figure 12. In both runs made with this injection system, dark areas continuously streamed from the tip of each impingement plate. A large dark pocket also remained at the entrance to the nozzle and another near the injection plate.

Two pair of intersecting jets. - When the impingement plates were removed from the Enzian injection system leaving two sets of single intersecting jets, the thrust remained quite low in each of two runs. The combustion during these runs is shown in figure 13. Run 17 appears quite similar to those with the Enzian injection system, whereas run 18 shows an unusual separation along the center of the chamber.

Premixing jets. - When the premixing-type nozzles were used, the run started in the usual manner and steady combustion was reached in about 0.16 second. Combustion was quite normal for about the next 0.14 second and then the propellant mixture in the injectors detonated and demolished the injectors and connecting tubes. A period of intense brightness existed throughout the entire combustion chamber lasting about 5 milliseconds at the time of the explosion. The combustion chamber itself suffered no damage. During the apparently normal portion of the run, a dark area extended along the upper contour-plate edge of the chamber but at a slight distance from it, as can be seen in figure 14. A second run with the premixing-type injectors resulted in a similar explosion of the injectors but no combustion photographs were taken.

#### DISCUSSION

The various combustion photographs have shown that the flame front does not start at the intersection of the jets but extends close to the point where the propellants enter the chamber. With the multiple intersecting jets without the turbulence projections and with the Enzian-type injection, noticeable dark areas existed around the nozzle. With all other injection systems investigated, the flame seemed to extend to the injector faces.

All the injection systems investigated showed considerable nonuniformity of combustion. The single intersecting jets without the turbulence projections, the multiple intersecting jets with the turbulence projections, and the premixing jets gave the most uniform combustion patterns. Although the data are not sufficiently

extensive and accurate to determine the effect of the nonuniformity of combustion of rocket performance, the assumption that a uniform combustion is the most desirable is logical.

Most of the photographs showed a great deal of stratification at the throat and the plastic was burned to a lesser depth behind the dark streaks than behind the bright areas. This effect is demonstrated in figure 15 by comparing a photograph of the combustion during one of the runs with the plastic plate from that run. On one side of the nozzle throat, the flame burned completely through the 1/4-inch-thick inner plate and slightly into the backing plate; on the other side, the plastic was burned to a maximum depth of only 3/16 inch. The combustion photograph shows that the side having the large nonluminous area was the side that was not burned so deeply. Thus nonuniform flow through the nozzle with the possibility of asymmetric thrust forces is indicated.

The luminosity of the gases decreases very rapidly as the gases pass into the divergent section of the nozzle and is probably caused by a decrease in both temperature and density. Even though the flame outside the rocket engine appeared very bright to the naked eye, it was not bright enough to appear in the high-speed photographs. Figure 15 further shows that in the divergent section of the nozzle a pattern in which the Mach lines are discernable was burned into the plastic sides.

The plastic sides alone form an interesting record of the run by showing variations in the injector action by burning to a greater depth in line with some of the propellant streams. If such burning occurs more on one plate than the other, poor alinement of the propellant streams is indicated. The sides also show some of the flow variations particularly around the turbulence projections and in the nozzle region. In most cases, the nozzle throats were burned deeper at the edges than in the middle indicating either higher velocities or temperatures at the edges. In the divergent section of the nozzle, the Mach angle can be measured from the pattern formed there, thus giving an additional check on the calculated conditions. In the runs presented herein, however, conditions varied too greatly from the beginning to the end of the run for such a measurement to have much value.

For many of the runs, measurement of the velocity of the propellant gases was possible in the combustion chamber by observing the movement of a nonluminous pocket. With the use of this value along with measured values for the combustion-chamber pressure, weight flow, and area in accordance with the following equation, the

combustion temperature divided by the molecular weight of the products ( $T_c/m$ ) can be determined:

$$\frac{T_c}{m} = \frac{V_c P_c A_c}{WR} \quad (1)$$

where

$T_c$  combustion-chamber temperature

$m$  average molecular weight of combustion gases

$V_c$  gas velocity in combustion chamber

$P_c$  combustion-chamber pressure

$A_c$  combustion-chamber cross-sectional area

$W$  total propellant weight flow

$R$  universal gas constant

In these experiments, the cross-sectional area and combustion-chamber pressure continually changed and there was insufficient timing correlation to determine values for the pressure and the area at the exact time for which the velocity was measured. These measurement uncertainties allow only an approximate measurement of  $T_c/m$  by the use of equation (1). The ratio  $T_c/m$  can be determined from other measured quantities, thus

$$\frac{T_c}{m} = \left( V_c \frac{A_c}{A_t} \right)^2 \left[ \frac{M^2(\gamma-1) + 2}{\gamma+1} \right]^{-\frac{\gamma+1}{\gamma-1}} \frac{1}{\gamma g R} \quad (2)$$

where

$A_t$  nozzle-throat area

$M$  combustion-chamber Mach number

$\gamma$  ratio of specific heats

$g$  acceleration due to gravity

Equation (2) can be derived from Bernoulli's equation by assuming an isentropic process. The ratio of specific heats cannot be experimentally measured but the use of the theoretical value of the ratio of specific heats introduces only a small error. For most rocket engines, the effect of combustion-chamber Mach number is so small that it can be neglected. In the experiments reported, the nozzle-throat area varied greatly during the runs and consequently the use of equation (2) to determine  $T_c/m$  is also subject to measurement uncertainties. The rapid erosion of the throat could be prevented by the use of an all-metal throat section at the sacrifice of the view of the throat but this possibility was not tried. The following table presents the ratio of the measured values of  $T_c/m$  as determined by the use of equations (1) and (2) to the theoretical values of  $T_c/m$ :

Run	Injection System	Theoretical $T_c/m$	Measured $T_c/m$ Theoretical $T_c/m$	
			Equation (1)	Equation (2)
3	Single intersecting jets with turbulence projections	244	0.57	0.46
8	Multiple intersecting jets without turbulence projections	250	0.46	0.39
16	Enzian injector	260	0.71	0.65

The areas used for the values shown in the table were those for the start of the run. Other values used were taken at the maximum combustion-chamber pressure. During each run the nozzle-throat area changed by a factor of 2, hence the measurement uncertainties for the variables of equation (1) were probably less than those for equation (2). By use of equation (1), the results show that the measured  $T_c/m$  varies from about 50 to about 70 percent of the theoretical  $T_c/m$ .

When  $T_c/m$  is known, computation of the speed of sound through the combustion gases and thus the various natural frequencies of the chamber is easy. By the use of an average value of  $T_c/m$  as obtained by means of equation (1) and a theoretical value for the ratio of specific heats, the following values were determined for the natural frequencies of the combustion chamber:

Dimension	Frequency (cps)
Length	1800
Width	6000
Thickness	33,000

982

On the combustion-chamber-pressure vibration records, two vibration frequencies were prominent throughout the runs: one at approximately 1900 cycles per second and the other at approximately 25,000 cycles per second. These vibrations therefore approximately correspond to the natural frequencies for the length and thickness of the chamber. Further investigations will be needed to verify this result.

Occasionally a frequency of about 4000 cycles per second was recorded and this frequency was found to be the natural frequency of the thrust stand. During the start of many of the runs, a distinct vibration of 100 to 300 cycles per second existed. This vibration corresponds to a brightening and dimming throughout the entire combustion chamber, as is shown in figure 7. Samples of the various vibration records are shown in figure 16.

#### SUMMARY OF RESULTS

The following results were obtained from an investigation of combustion of liquid oxygen and gasoline in a transparent-sided rocket engine:

1. The flame front did not start at the intersection of the propellant streams but extended almost to the faces of the injectors.
2. Combustion-chamber-pressure vibrations were recorded that approximately corresponded to the resonant frequencies of the length and thickness of the combustion chamber; these vibrations were the only definite frequencies recorded during the stable portion of the run.
3. All seven of the injection systems investigated showed considerable nonuniformity of combustion. The single intersecting jets without turbulence projections, the multiple intersecting jets with turbulence projections, and the premixing jets gave the most uniform combustion patterns.

4. The measured value for the combustion chamber temperature divided by the molecular weight of the combustion gases varied from about 50 to 70 percent of the theoretical value.

5. The luminosity of the combustion gases decreased very rapidly as they passed into the divergent section of the nozzle.

Flight Propulsion Research Laboratory,  
National Advisory Committee for Aeronautics,  
Cleveland, Ohio.



CONFIDENTIAL

NACA RM No. E8F01

TABLE I - EXPERIMENTAL AND CALCULATED DATA FOR COMBUSTION

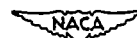
Run	Injection system	Number of turbulence projections	Peak thrust (lb)	Photographic data at approximately			
				Time from fuel start (sec)	Gasoline flow (lb/sec)	Liquid-oxygen flow (lb/sec)	Total propellant flow (lb/sec)
1	Single intersecting jets	0	75	-----	-----	-----	-----
2	Do. - - - - -	2	53	0.63	0.174	0.298	0.472
3	Do. - - - - -	2	109	1.18	.173	.313	.486
4	Do. - - - - -	2	96	1.48	.156	.325	.481
5	Multiple intersecting jets	0	58	1.25	.171	.325	.496
6	Do. - - - - -	0	98	.87	.173	.470	.643
7	Do. - - - - -	0	112	1.10	.167	.495	.662
8	Do. - - - - -	0	84	.86	.173	.340	.513
9	Do. - - - - -	0	-----	.96	.175	.570	.740
10	Do. - - - - -	0	91	1.10	.171	.350	.521
11	Do. - - - - -	0	110	1.28	.161	.445	.606
12	Do. - - - - -	2	113	.89	.178	.346	.524
13	Do. - - - - -	2	-----	1.08	.178	.352	.530
14	Do. - - - - -	2	72	.74	.179	.232	.411
15	Enzian	2	(d)	1.28	.177	.240	.417
16	Do. - - - - -	2	115	1.27	.175	.416	.591
17	Two pair of intersecting jets	0	73	1.50	.178	.240	.418
18	Do. - - - - -	0	65	1.40	.157	.212	.367
19	Premixing <sup>c</sup>	0	-----	1.33	.158	.397	.555

<sup>a</sup>When no combustion-chamber pressure was recorded, data recorded about 1 second after start are shown.

<sup>b</sup>Specific impulses were calculated on only propellant flows and did not consider weight of plastic consumed.

<sup>c</sup>Injectors exploded during run.

<sup>d</sup>Approximately 100 pounds.



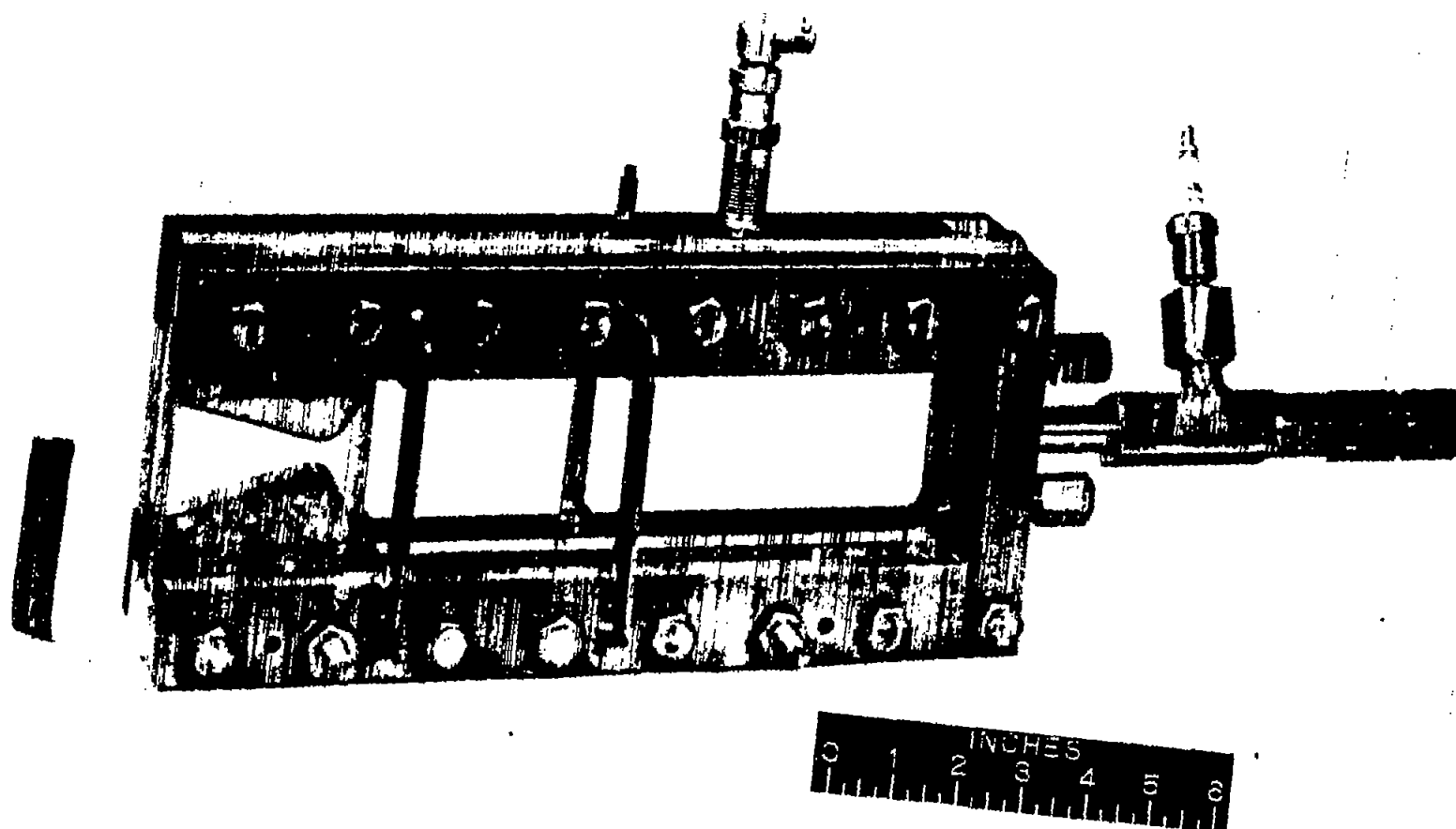
## OF LIQUID OXYGEN AND GASOLINE IN TRANSPARENT-SIDED ROCKET

maximum combustion-chamber pressure <sup>a</sup>			Oxygen-gasoline ratio	Specific impulse <sup>b</sup> (sec)	Initial throat area (sq in.)	Characteristic velocity (ft/sec)
Liquid-oxygen injection pressure (lb/sq in.)	Gasoline injection pressure (lb/sq in.)	Combustion-chamber pressure (lb/sq in.)				
187	316	122	1.72	112	0.256	2420
316	456	230	1.81	224	.254	3910
220	298	180	2.18	200	.274	3600
275	305	194	1.90	117	.288	3950
363	360	228	2.72	152	.285	3500
370	350	223	2.97	169	-----	-----
305	360	230	1.97	164	-----	-----
350	190	-----	3.26	-----	-----	-----
290	340	215	2.05	175	.259	3720
370	300	242	1.77	182	-----	-----
273	313	-----	1.94	216	.284	-----
238	184	-----	1.98	-----	-----	-----
250	278	173	1.30	175	.259	3870
290	600+	196	1.36	-----	-----	-----
366	600+	246	2.38	195	.260	3730
236	600+	176	1.35	175	.258	3850
232	554	164	1.35	176	-----	-----
170	218	50	2.52	-----	.263	1000

NACA

1874

1875

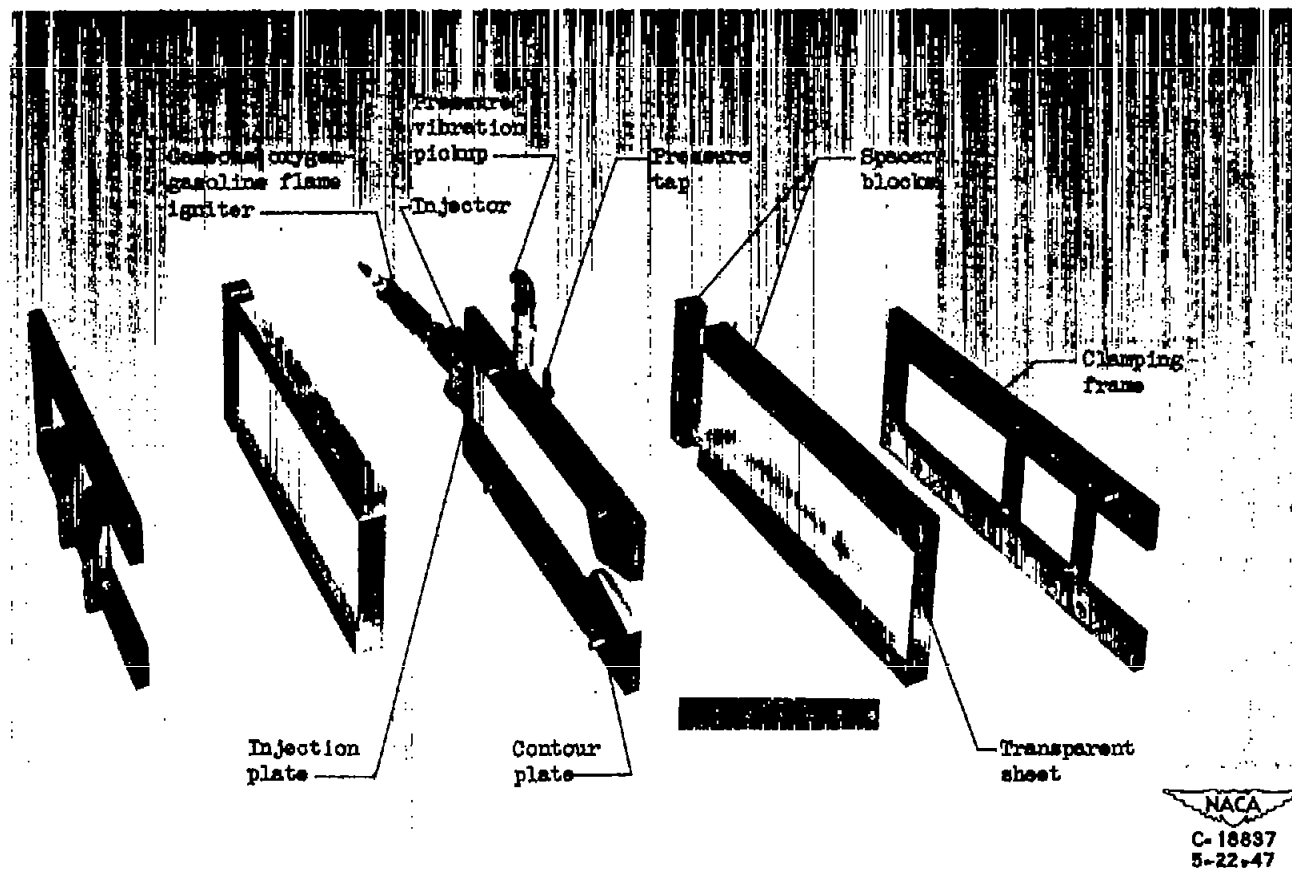


NACA  
C-18838  
5-22-47

(a) Assembled.  
Figure 1. - Transparent-sided rocket engine equipped with single-impinging jets and gaseous oxygen - alcohol igniter.

100

100



(b) Unassembled.

Figure 1. - Concluded. Transparent-sided rocket engine equipped with single-impinging jets and gaseous oxygen - alcohol igniter.

100

100

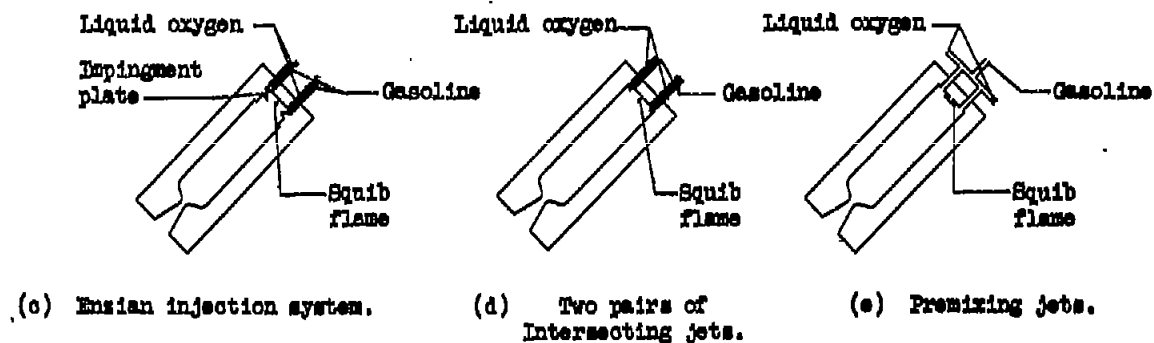
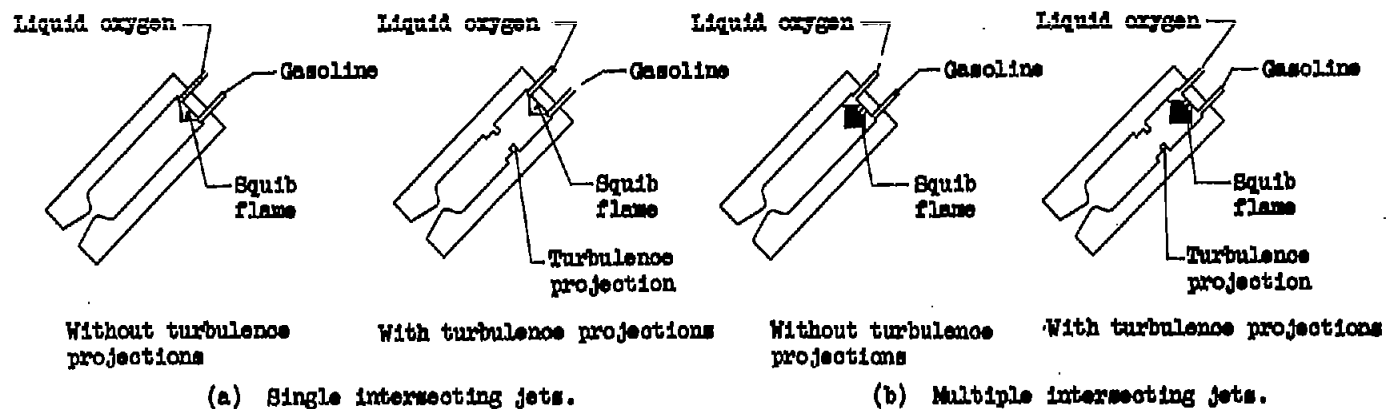


Figure 2. - Diagrammatic sketches of seven propellant injection systems.

NACA  
C-20559  
3-8-48



1871

1

2

3

4

5

6

7

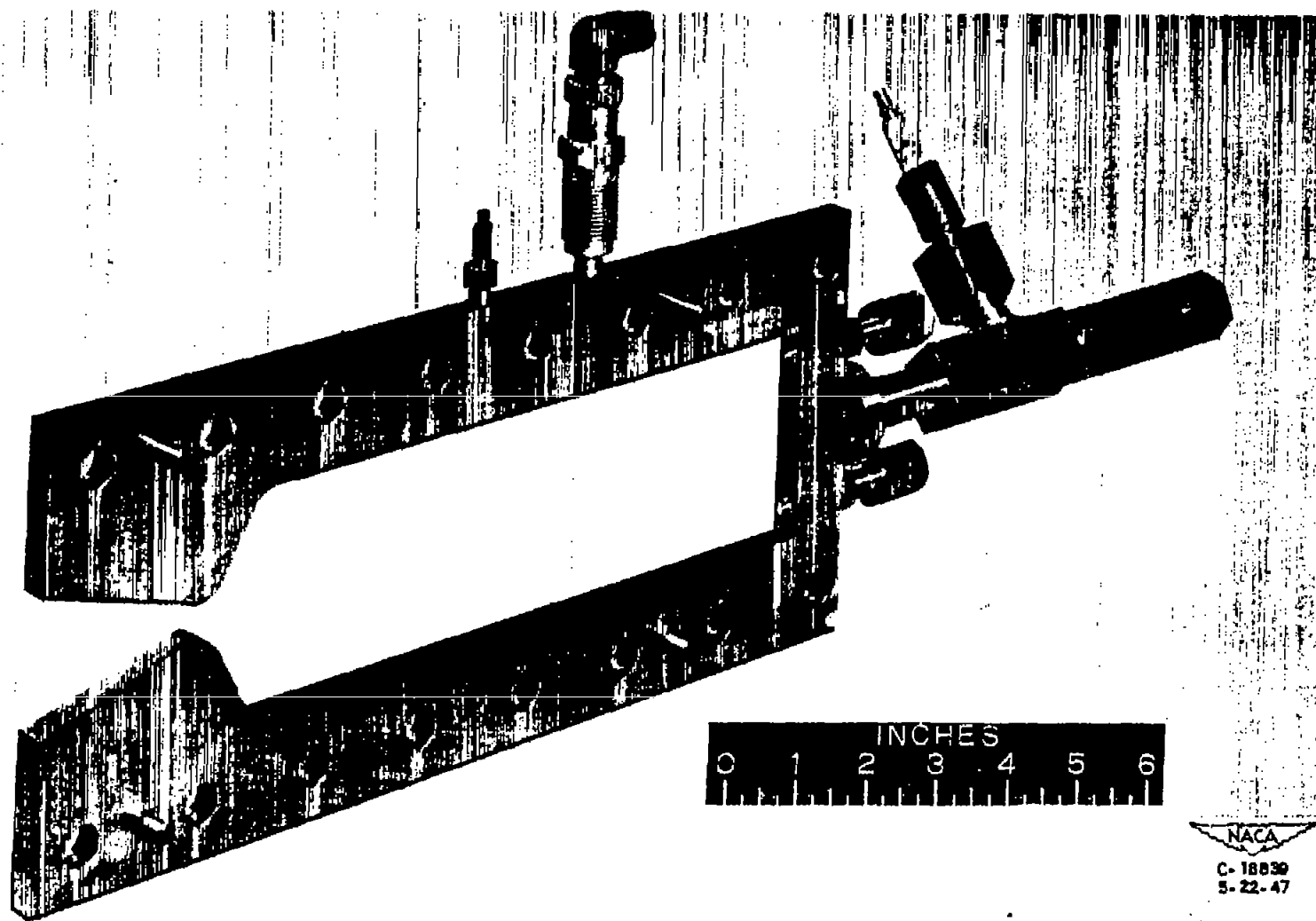


Figure 3. - Contour and injection plates equipped with single-intersecting jets and gaseous oxygen - alcohol igniter.

100

100

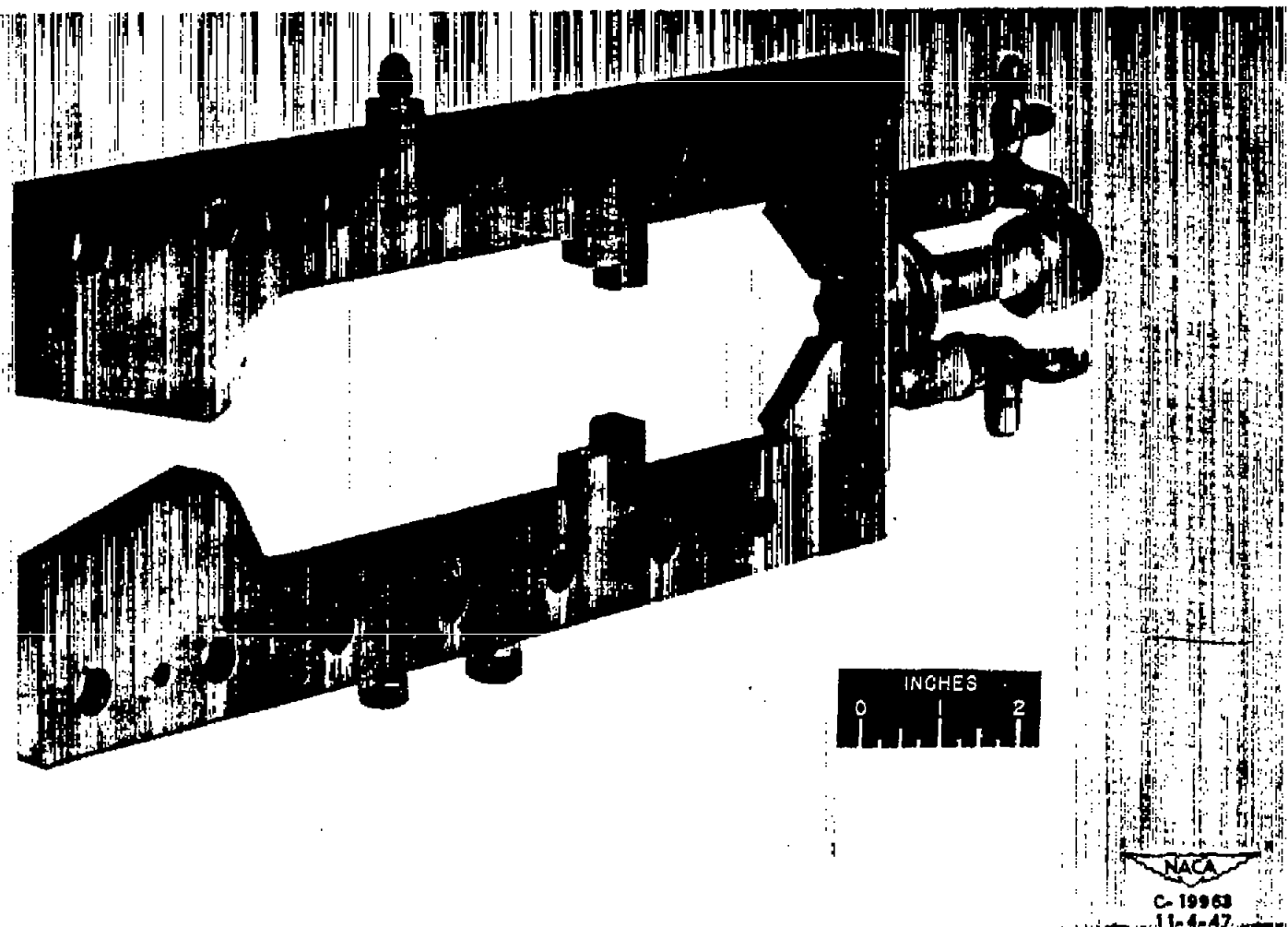
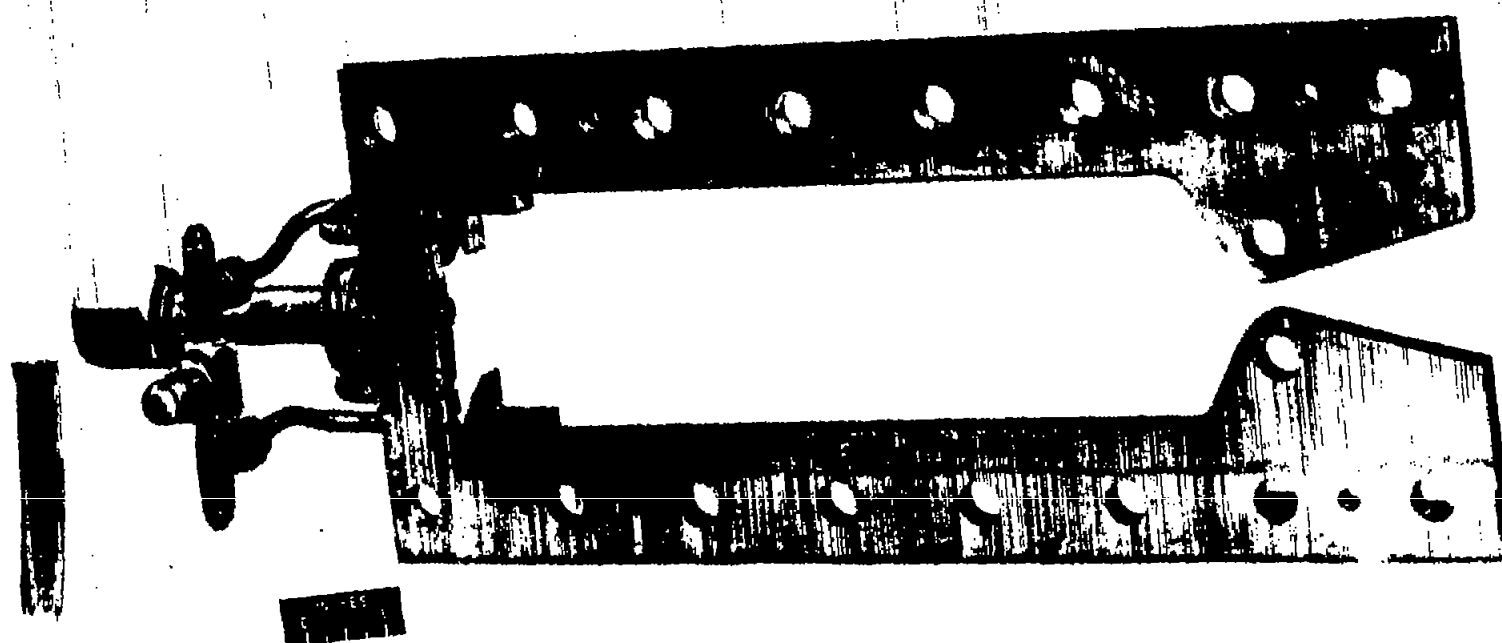


Figure 4. - Contour and injection plates equipped with multiple-intersecting jets, turbulence projections, and squib igniter.

100

100



NACA  
C-20378  
12-30-47

Figure 5. - Contour and injection plates equipped with Enzian-type injectors and equib igniter.

1000

1000

1000

1000

1000

1000

1000

1000

1000

1000

1000

1000

- A Secondary oxygen pressure regulator
- B Primary oxygen pressure regulator
- C Oxygen-supply pressure gage
- D Filter
- E Three-way air-operated valve
- F Three-way solenoid valve
- G Liquid-oxygen flowmeter dial
- H Combustion-chamber pressure gage
- I Gaseous-oxygen supply tank
- J Clock
- K Liquid-oxygen-tank pressure gage
- L Liquid-oxygen tank
- M Gasoline-nozzle pressure gage
- N Liquid-oxygen-nozzle pressure gage
- O Rotameter
- P Data camera
- Q Gasoline-pump pressure gage
- R Pressure tap
- S Pressure vibration pickup
- T Liquid-oxygen flowmeter element
- U Two-way air-operated valve
- V Combustion chamber
- W Squib
- X Propellant control valve - liquid oxygen
- Y Actuating air cylinder
- Z Propellant control valve - gasoline
- AA Small pressure tank
- BB Hydraulic resistance
- CC Relief valve
- DD Gasoline pumps
- EE Electric motor
- FF Secondary nitrogen pressure regulator
- GG Primary nitrogen pressure regulator
- HH Nitrogen filling connection
- II Gasoline tank
- JJ Nitrogen supply tank

Shaded area shows instruments recorded by data camera

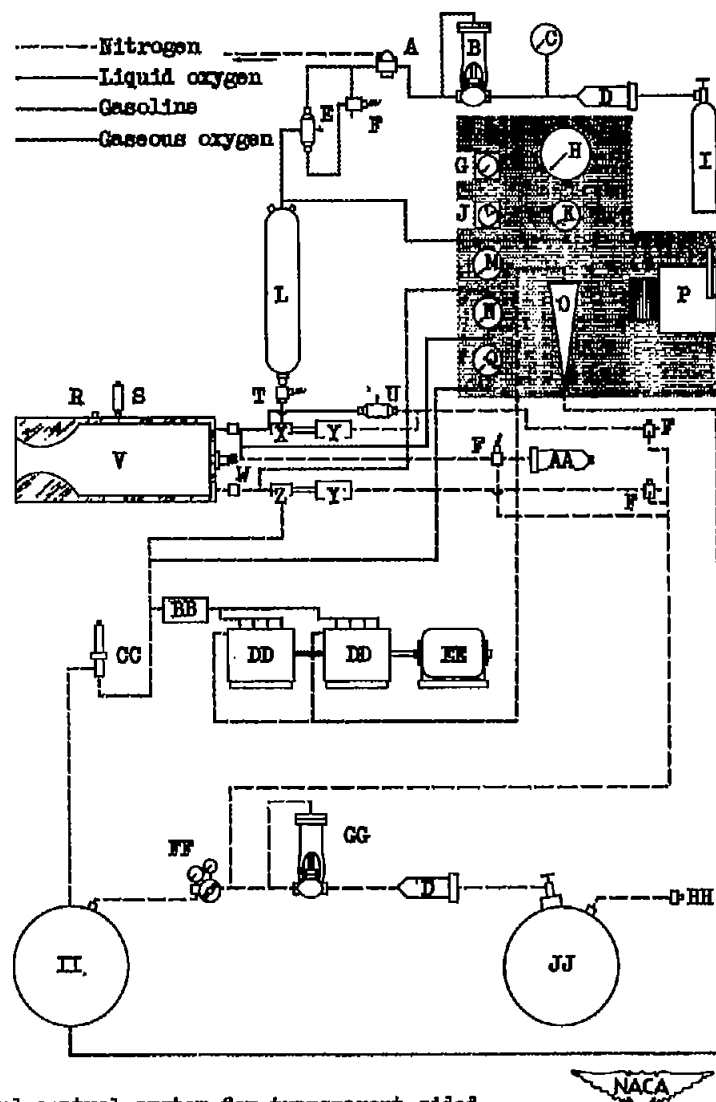
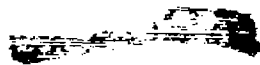
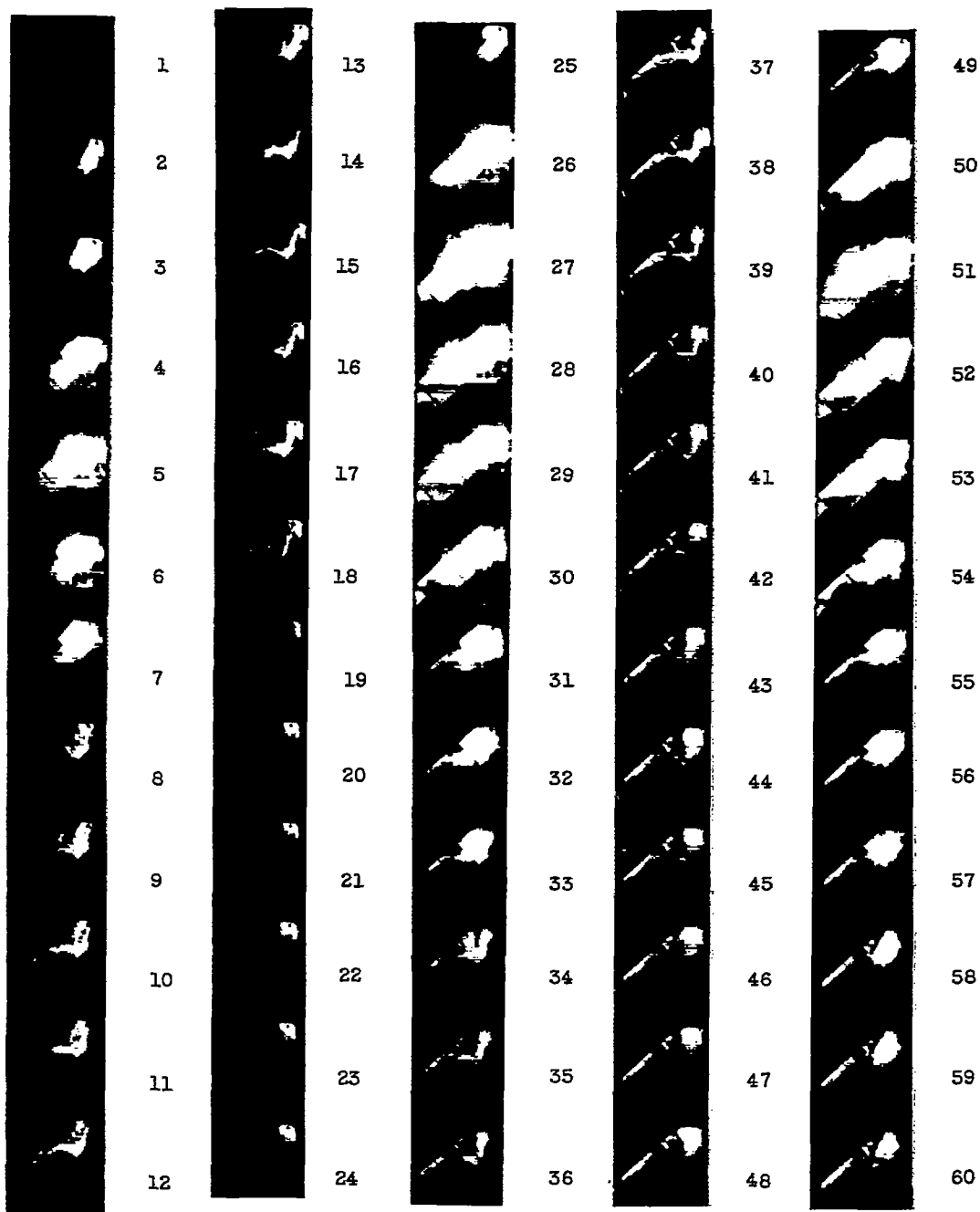


Figure 6. - Diagrammatic sketch of propellant and control system for transparent-sided rocket engine.





Frame



NACA  
C-21539  
5-26-48

Figure 7. - Starting explosions in transparent-sided rocket engine using liquid oxygen and gasoline and having multiple-intersecting jets with turbulence projections. Run 14; interval between frames, 1.66 milliseconds at frame 1 decreasing to 1.44 milliseconds at frame 60.

1

2

3

4

5

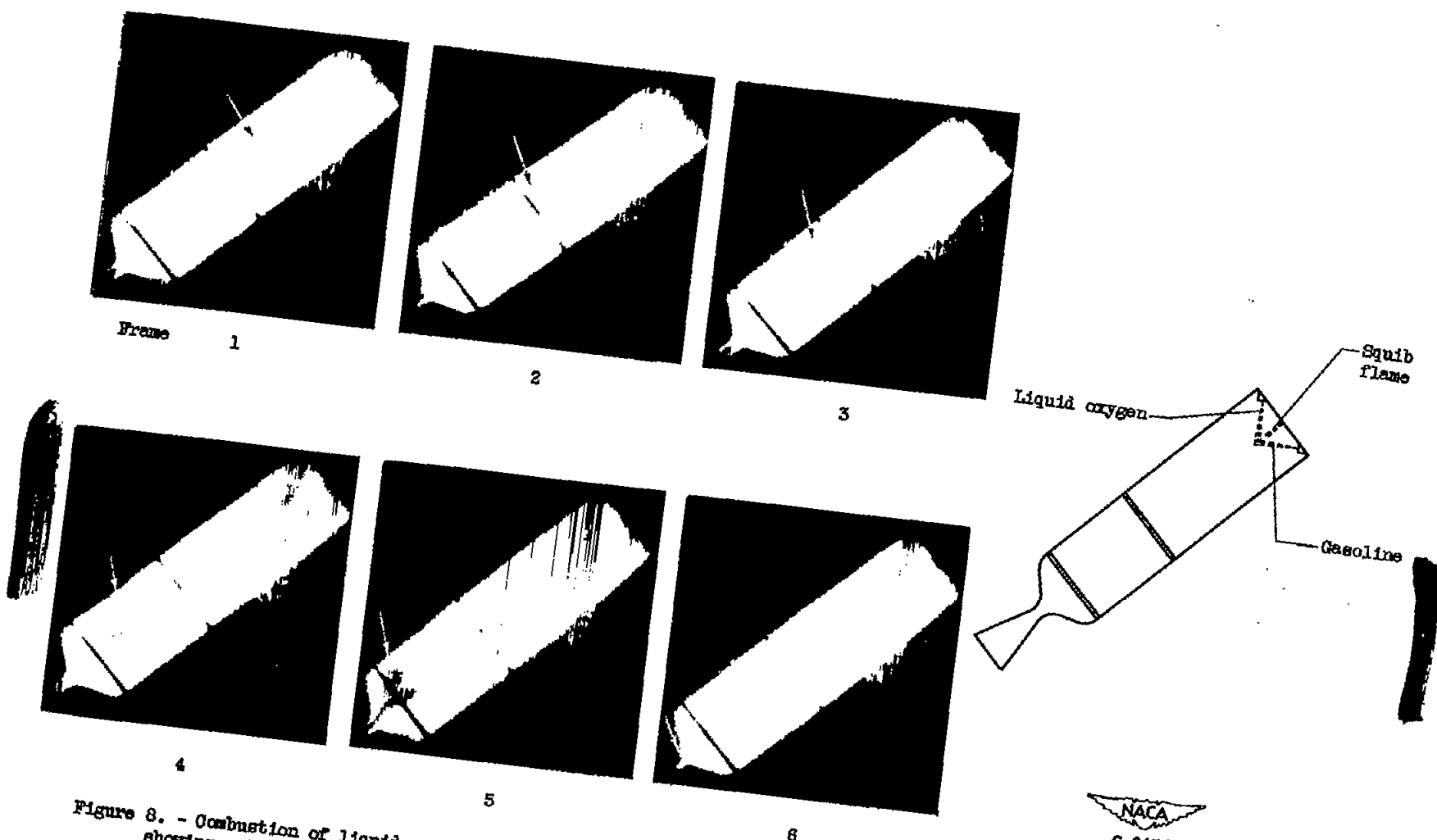
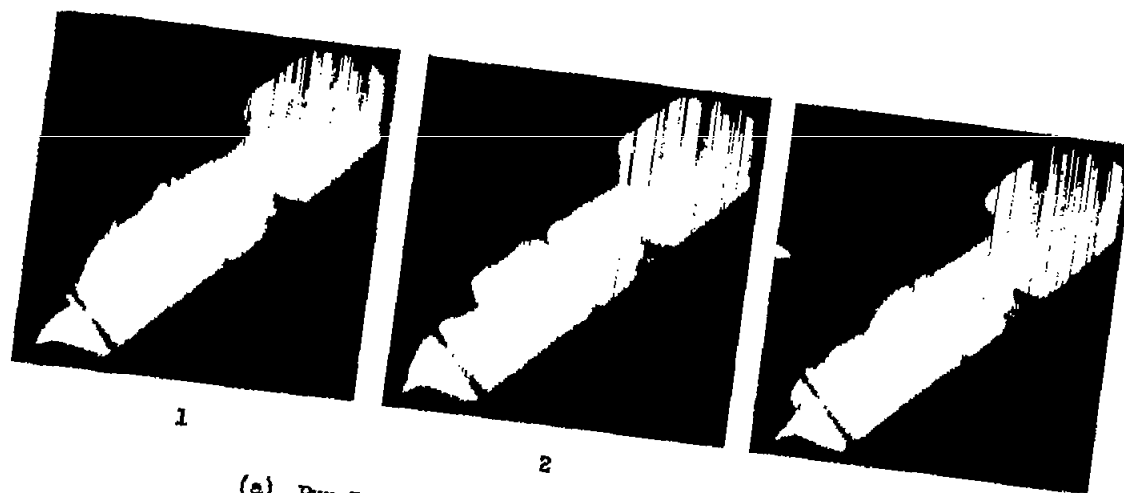


Figure 8. - Combustion of liquid oxygen and gasoline in transparent-sided rocket engine using single-intersecting jets and showing motion of nonluminous pocket. Run 1; interval between frames, 0.333 millisecond; thrust, 75 pounds.

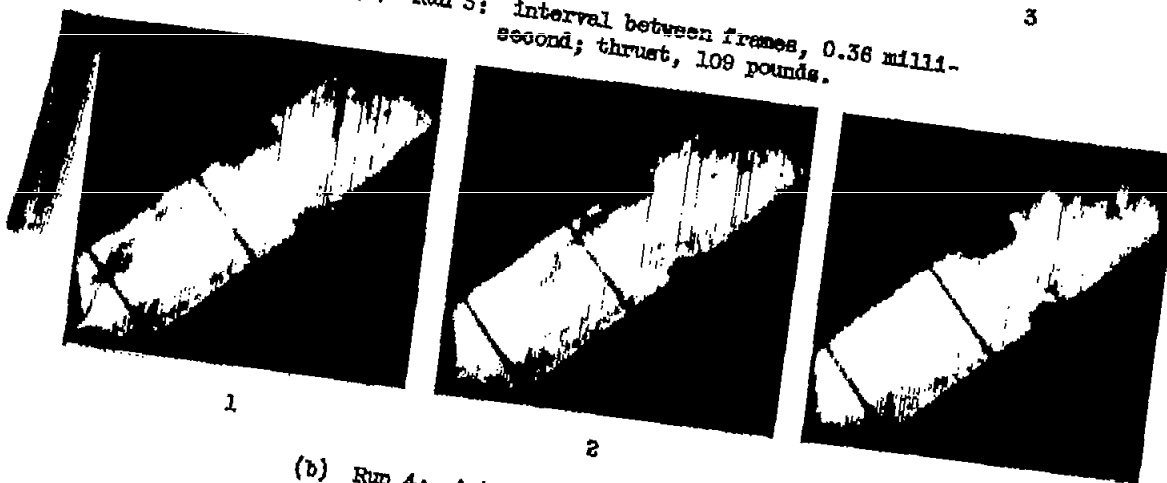
NACA  
C-21540  
5-26-48

1875

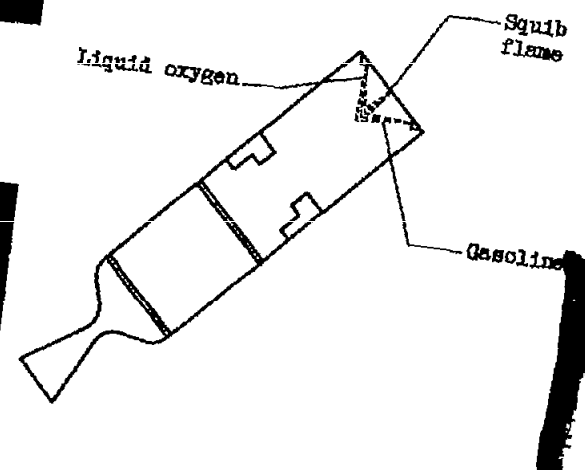
1875



(a) Run 3: interval between frames, 0.36 milli-second; thrust, 109 pounds.



(b) Run 4: interval between frames, 0.316 milli-second; thrust, 96 pounds.

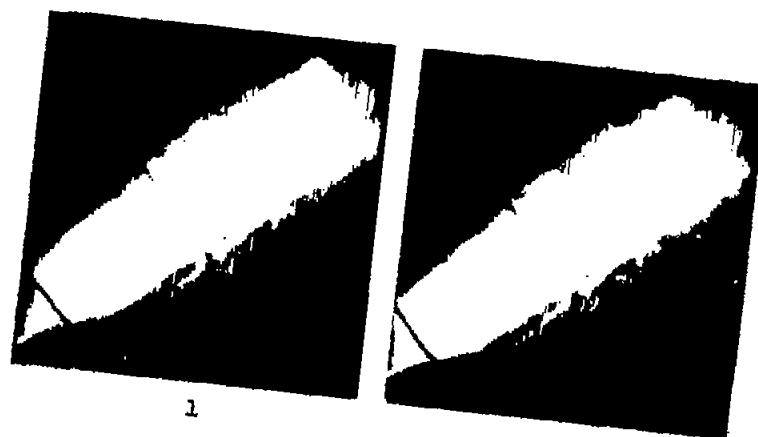


NACA  
C-21541  
5-26-48

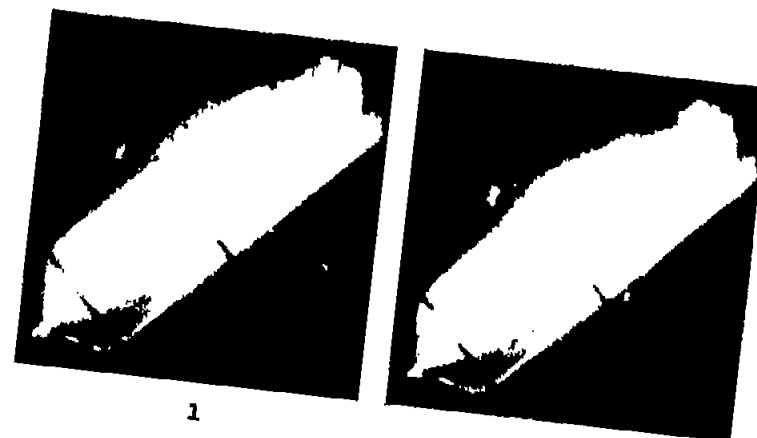
Figure 9. - Combustion of liquid oxygen and gasoline in transparent-sided rocket engine using single-intersecting jets with turbulence projections.

1871

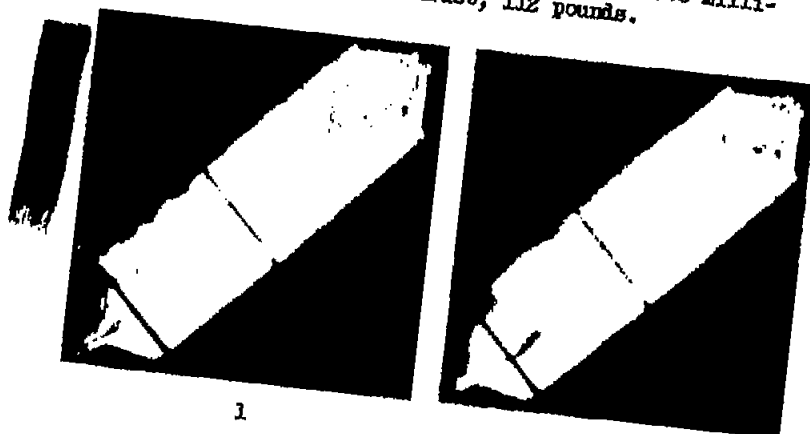
1872



(a) Run 7: interval between frames, 0.353 milli-second; thrust, 112 pounds.



(b) Run 8: interval between frames, 0.356 milli-second; thrust, 84 pounds.



(c) Run 10: interval between frames, 0.374 milli-second; thrust, 91 pounds.

NACA  
C-21542  
5-26-48

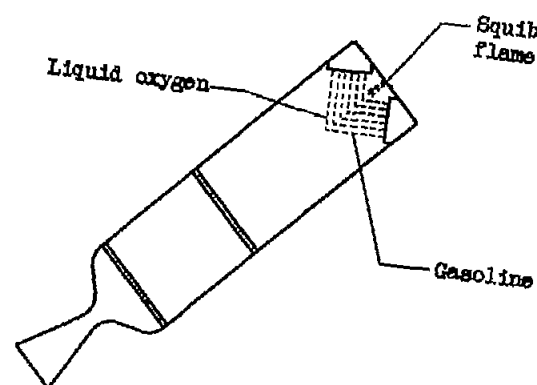
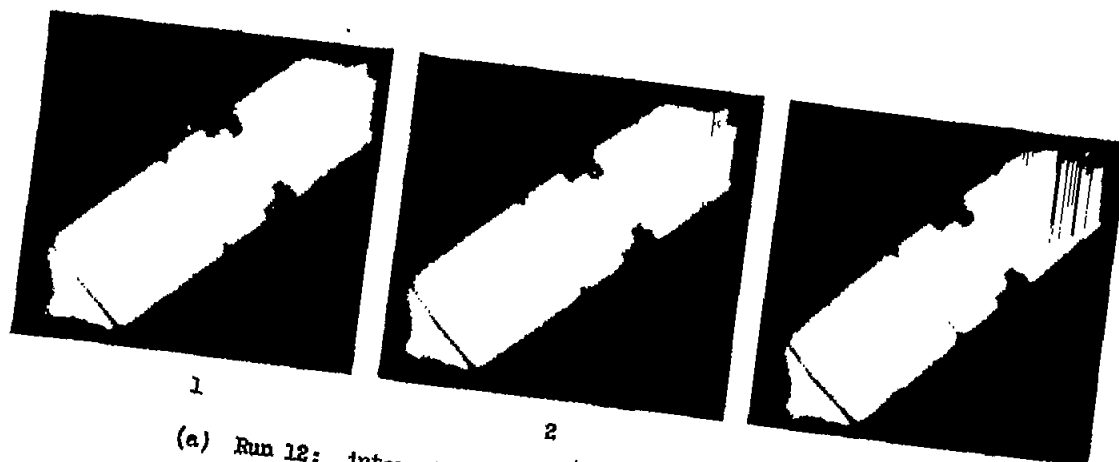


Figure 10. - Combustion of liquid oxygen and gasoline in transparent-sided rocket engine using multiple-intersecting jets.

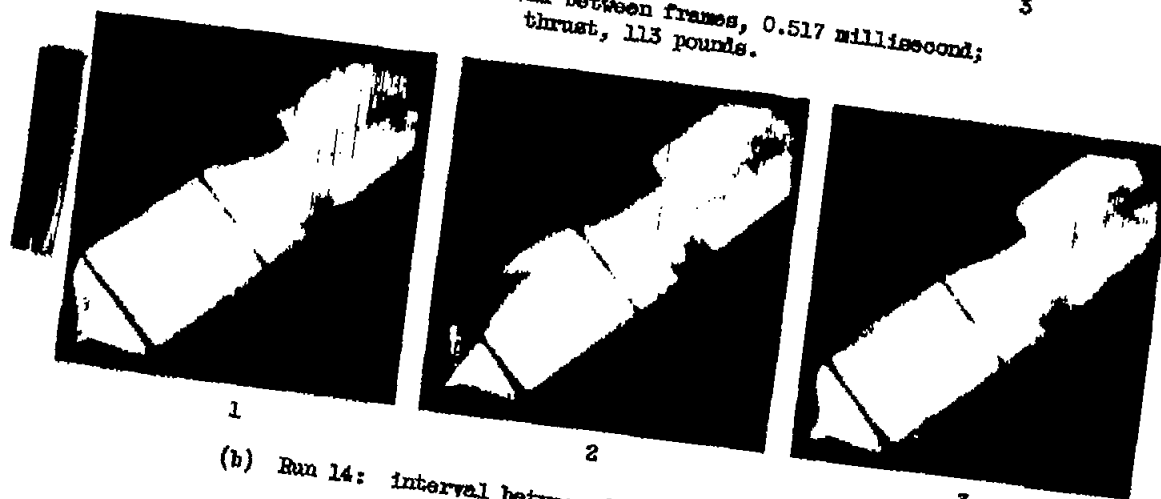


100

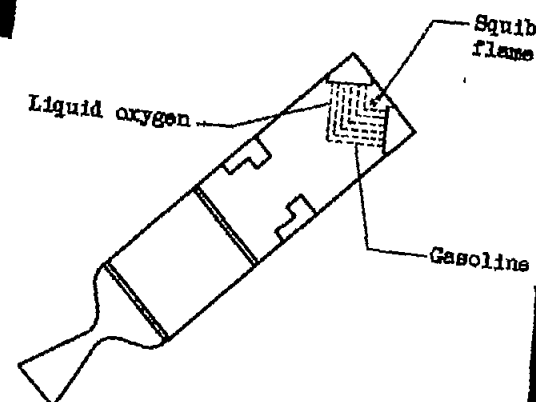
100



(a) Run 12: interval between frames, 0.517 millisecond;  
thrust, 113 pounds.



(b) Run 14: interval between frames, 0.402 millisecond;  
thrust, 72 pounds.

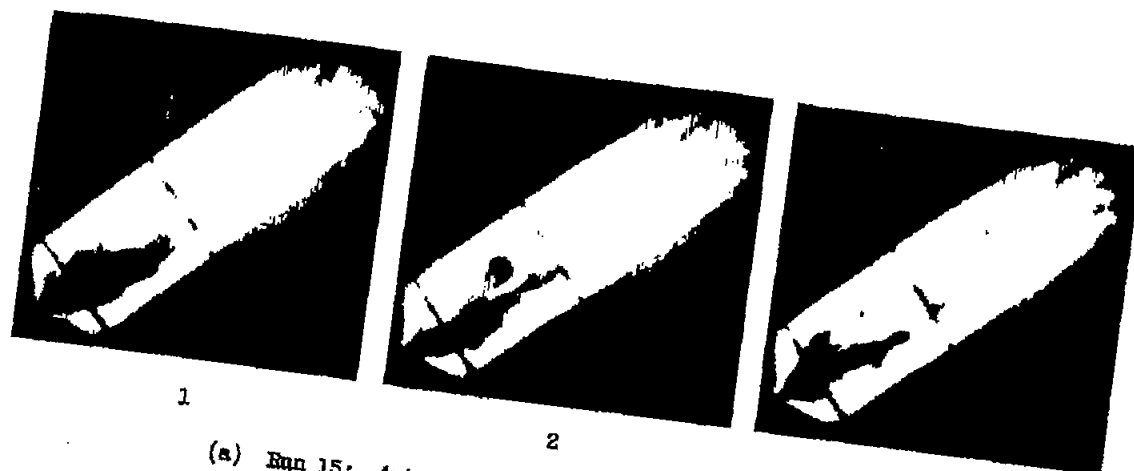


NACA  
C-21543  
5-26-48

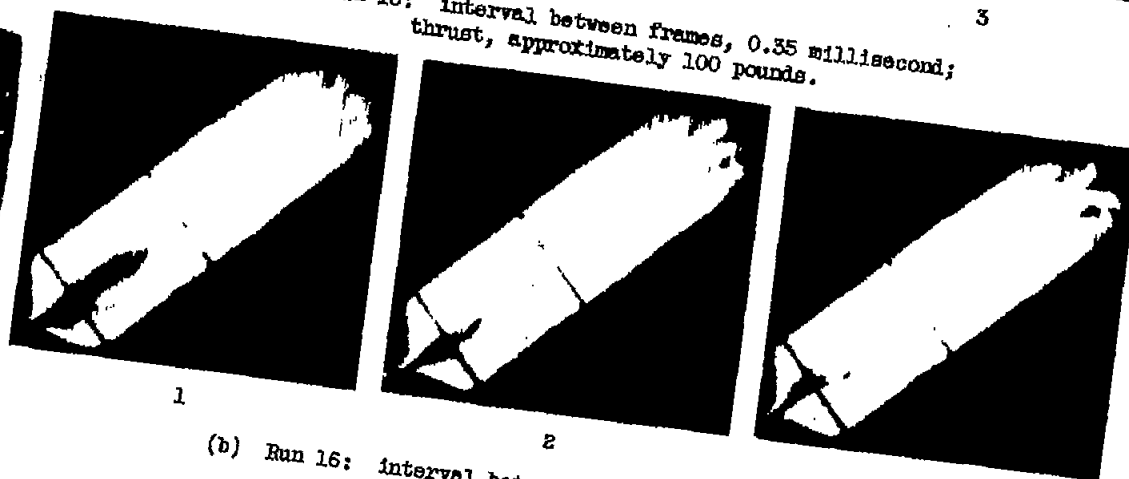
Figure 11. - Combustion of liquid oxygen and gasoline in transparent-sided rocket engine using multiple-intersecting jets with turbulence projections.

1944

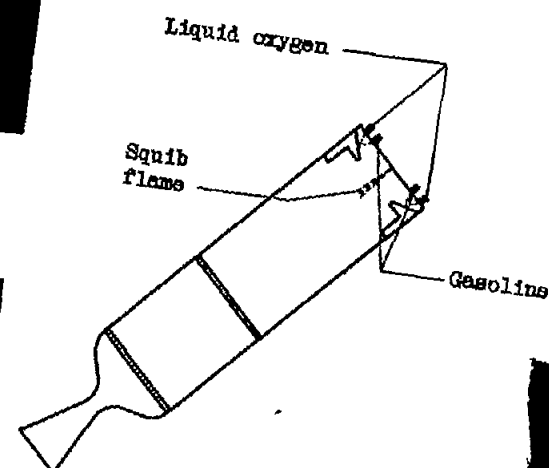
1944



(a) Run 15: interval between frames, 0.35 millisecond;  
thrust, approximately 100 pounds.



(b) Run 16: interval between frames, 0.34 millisecond;  
thrust, 115 pounds.

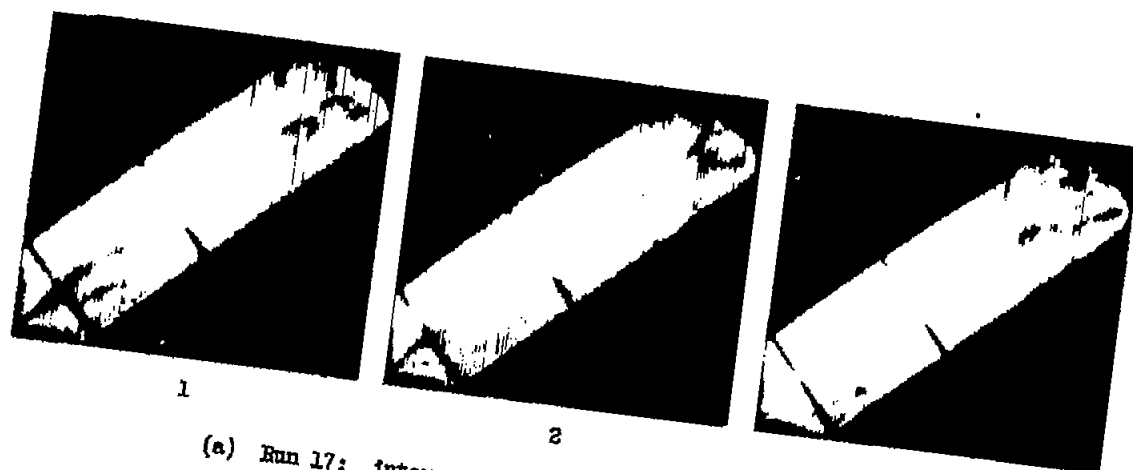


NACA  
C-21544  
5-26-48

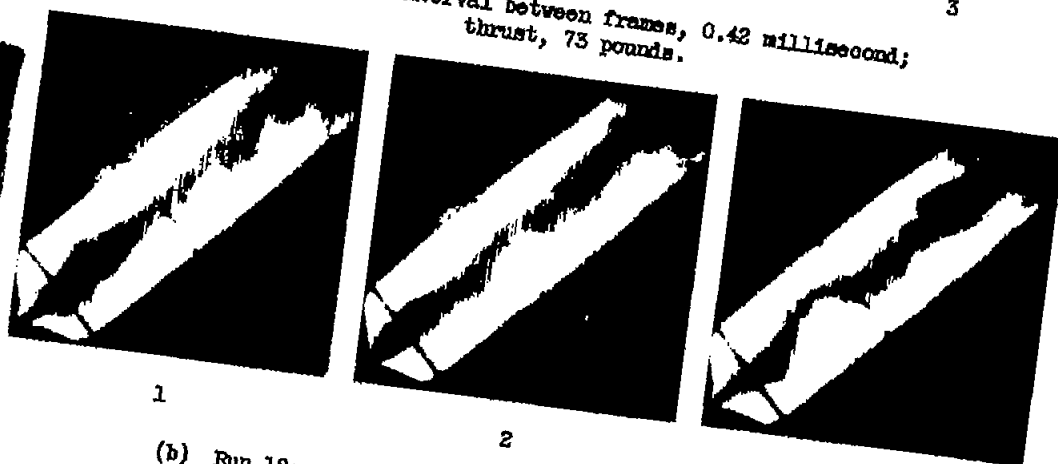
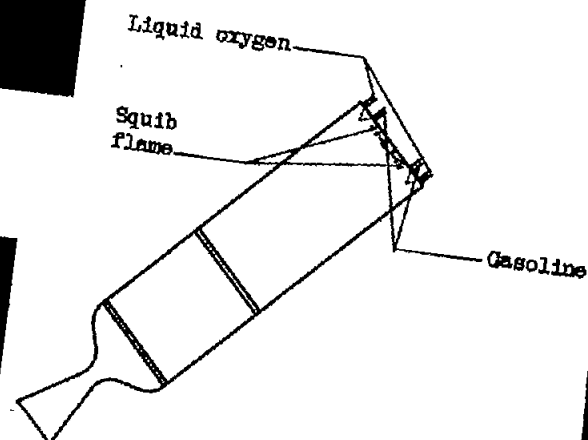
Figure 12. - Combustion of liquid oxygen and gasoline in transparent-sided rocket engine using Enxian injection system.

1000

1000



(a) Run 17: interval between frames, 0.42 millisecond;  
thrust, 73 pounds.



(b) Run 18: interval between frames, 0.36 millisecond;  
thrust, 65 pounds.

NACA  
C-21545  
5-26-48

Figure 13. - Combustion of liquid oxygen and gasoline in transparent-sided rocket engine using two sets of single-intersecting jets.

100

100

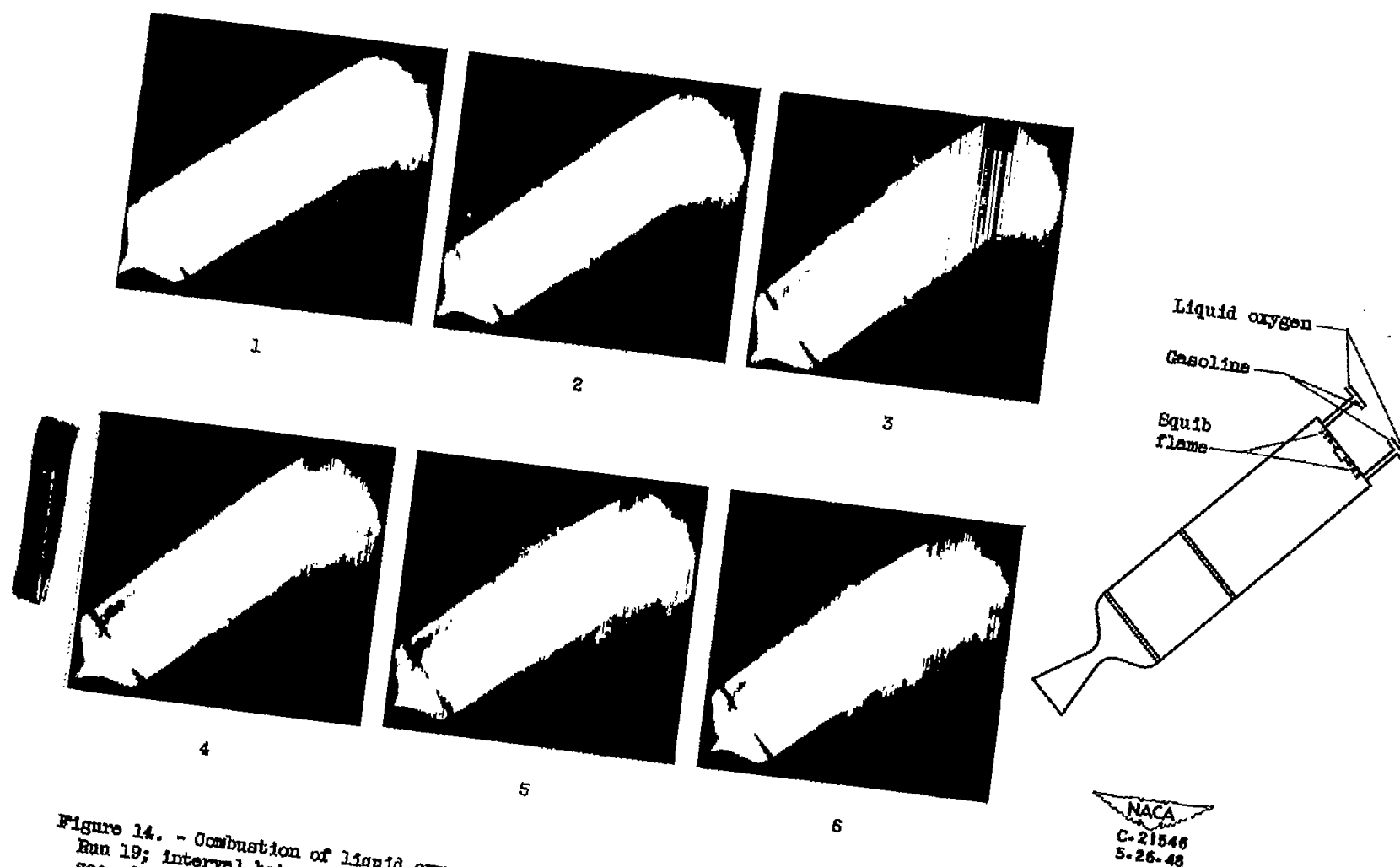
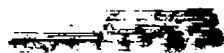
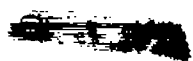
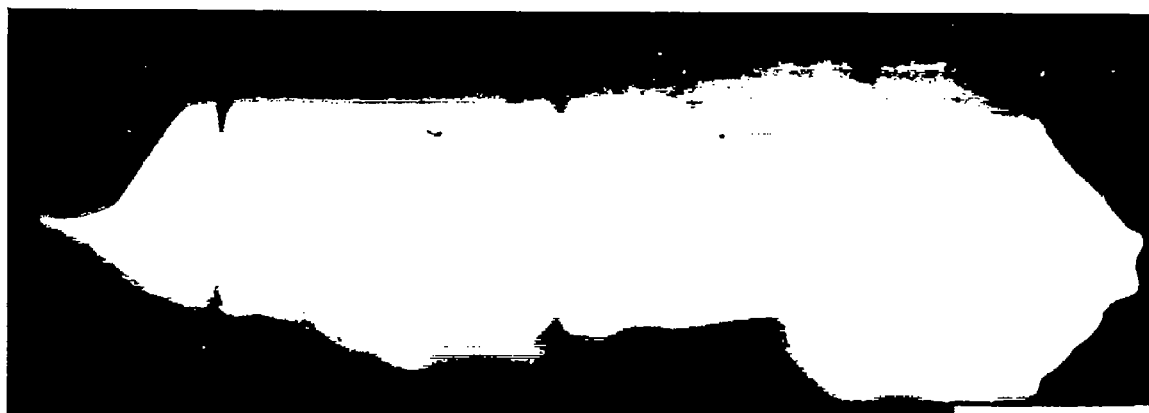
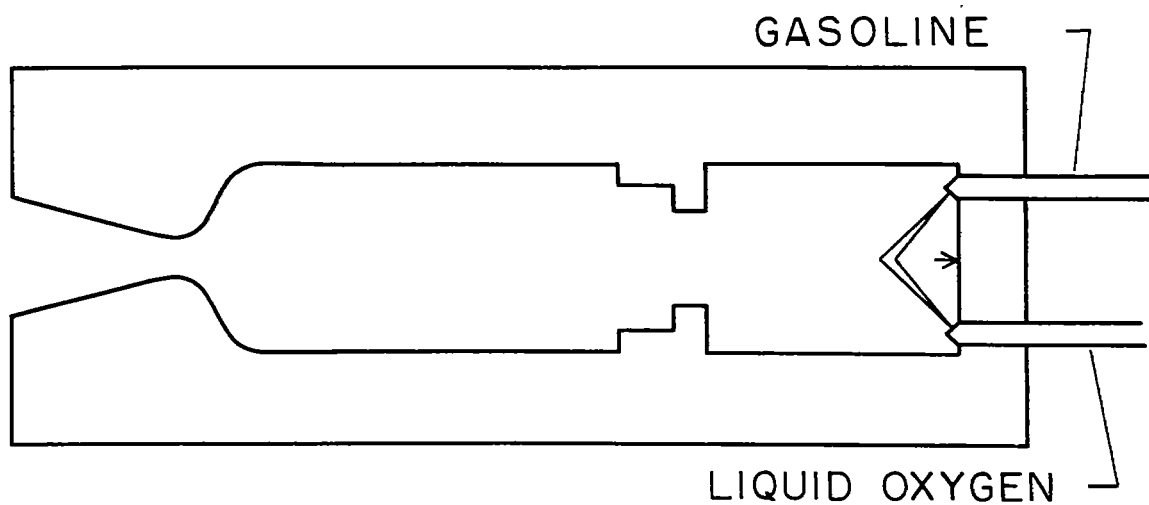


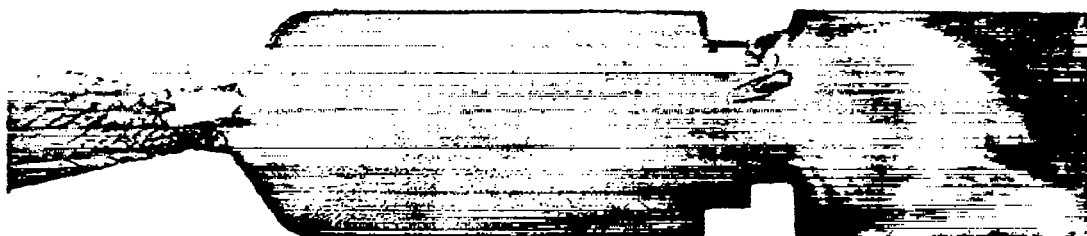
Figure 14. - Combustion of liquid oxygen and gasoline in transparent-sided rocket engine using two premixing-type injectors. Run 19; interval between frames, 0.35 millisecond; thrust not recorded (propellant mixture in injectors detonated 84 milli-sec after these photographs were taken).







NACA  
C-20950  
3-25-48



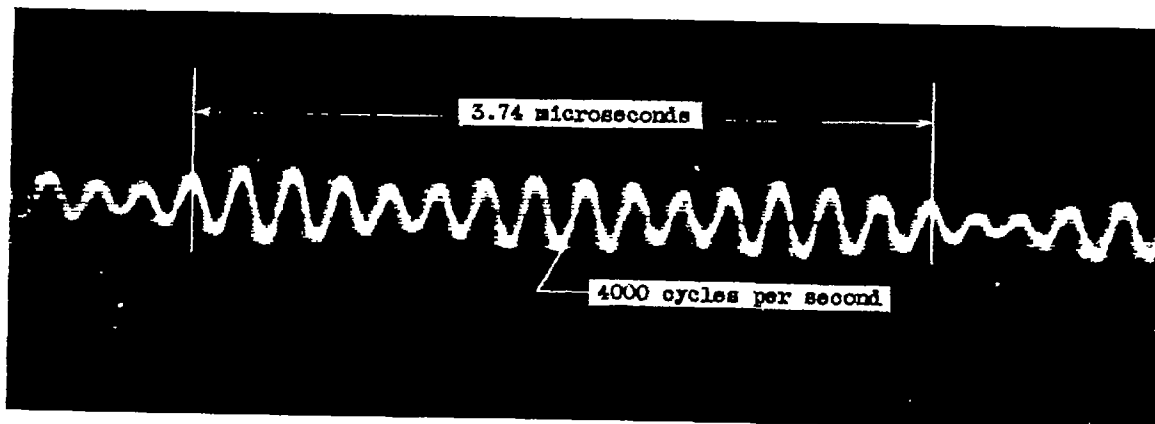
NACA  
C-20377  
12-30-47



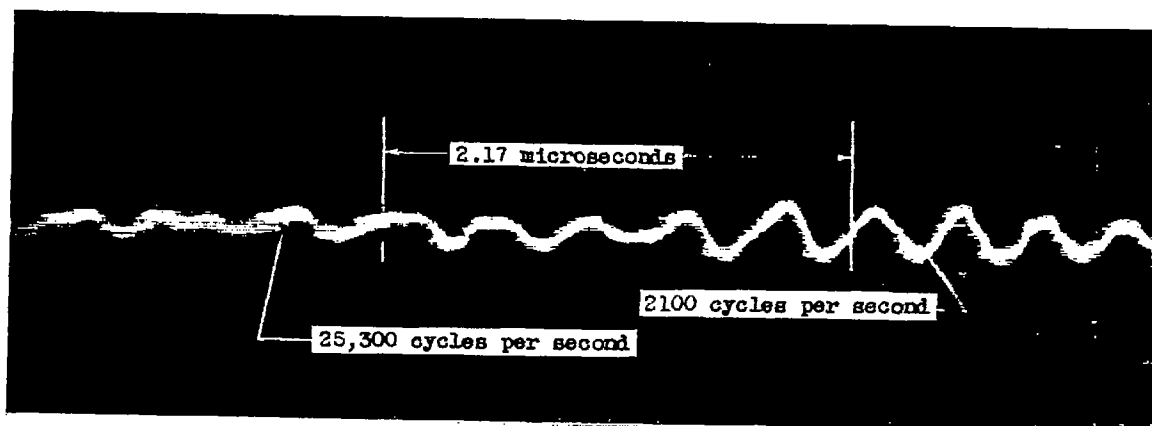
Figure 15. - Plastic plate after run of 1.9 seconds and combustion photograph taken through same plate. Run 3.

[REDACTED]

[REDACTED]

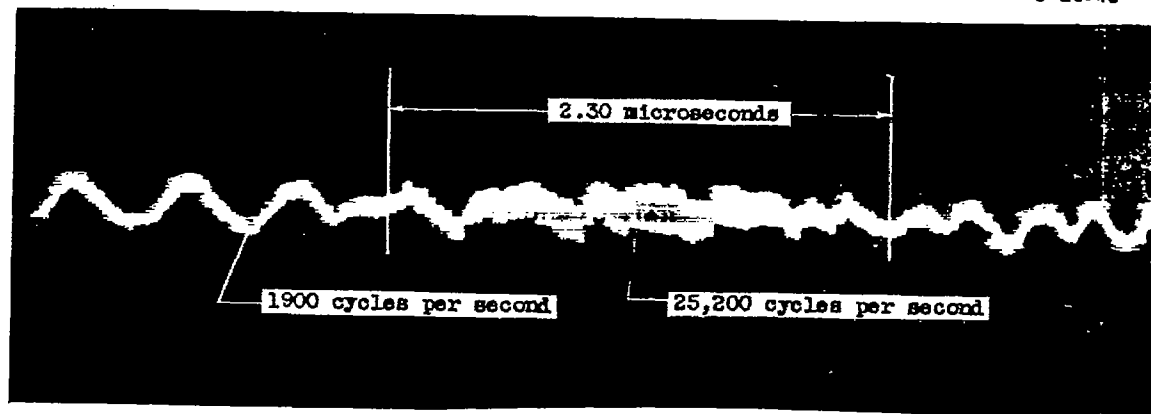


(a) Before start of run.



(b) After start of run.

NACA  
C-21547  
5-26-48



(c) Near end of run.

Figure 16. - Combustion-chamber-pressure vibration records using a magnetostriction-type pressure pickup. Run 11.